Recent Advances of Wearable Sweat-Sensing Devices

Subjects: Engineering, Biomedical | Engineering, Electrical & Electronic

Contributor: Nur Fatin Adini Ibrahim , Norhayati Sabani , Shazlina Johari , Asrulnizam Abd Manaf , Asnida Abdul Wahab , Zulkarnay Zakaria , Anas Mohd Noor

A sweat-sensing device requires a wearable device for the temporary attachment of its main components, including sensors, sweat collection devices, and electronic devices to the body's skin region.

sweat-sensing applications wearable device real-time measurement

1. Sweat-Sensing Device (SSD)

A sweat-sensing device requires a wearable device for the temporary attachment of its main components, including sensors, sweat collection devices, and electronic devices to the body's skin region. There are three primary types of wearable devices that are most commonly found in sweat applications: sweatbands [1], epidermal patches [2], and textiles [3]. Several factors to be considered in selecting which types of wearable devices are best suited for use in SSDs include the skin surface on a body location, sample collection techniques, and environmental conditions, whether on dry land or in aquatic exercise. For example, a sweatband is appropriate for wearing on specific body parts such as the wrist [4], arm [5], back [6], or forehead [7], where the bands can be tightened, as shown in **Figure 1**a. In addition, most of the literature prefers wearable sweatbands on the arm for cystic fibrosis tests during the conducting of conventional pilocarpine iontophoresis and sweat collection samples [8][9]. The band can be worn repeatedly with reusable electrodes during pilocarpine iontophoresis to trigger perspiration at any time due to the ease of detachment and reattachment of the electrodes from the band.

An epidermal patch is characterized by a disposable style of adhesive skin tape. It is low-cost, making it a practical SSD in a disposable format [10]. Wearable epidermal patches in SSDs typically come in various forms, such as skin patches [11], tattoos [12][13], and bandages [14][15], as shown in **Figure 1**b–d. The elements of substrate epidermal patches can promote strong skin adhesion, high mechanical strength, stretchability, and resilience in water conditions to manipulate physical skin performance. Moreover, an epidermal patch has a high flexibility for wearing on any part of the body's skin and a good adaptability in high-intensity exercise. Furthermore, they are versatile enough to be worn for use in water sports such as swimming [16]. Reeder et al. proposed an epidermal patch for colorimetric sensing integrated with microfluidic and water-proof electronic systems that can perform real-time physiological measurements on swimmers and dryland athletes [17]. In particular, most colorimetry sensing applies epidermal patches as wearable devices, as this device can be used for the single-shot measurement of sweat biomarkers once they change color, as reported by previous studies [18][19].

A textile-based sensor has advantages over sweatbands and epidermal patches in terms of substrate washability when exposed to humidity and dirt. Moreover, the textile can serve either as a sweat collection device by absorption or as a wearable device. Recent textile-based sensing devices have a fitted sensor on regular cloth such as a t-shirt [20][21], as shown in **Figure 1**e. Thus, they offer the advantages of being comfortable and allowing users to wear in any regular clothes. Recently, some SSDs have been woven with sensor and electronic components into highly stretchable fibers, making them suitable for applications requiring high-motion applications. The detection of motion and physiological signals by a fitted sensor into a t-shirt also enable the easy examination of numerous physiological valuable data, including a person's movement for the detection of Parkinson's disease and stress levels [22][23][24]. Recently, several technologies and materials used in textile-based sensing devices have been improved to ensure they can operate under intense mechanical tension during regular activities and be reused without interfering with the analytical performance of a sensor after washing. Wicaksono et al. [20] and Martinez-Estrada et al. [25] developed a highly robust sensor-based textile that integrates with electronic component reusability after washing. A smart textile comprises water-resistant and detachable electronics for the convenience of washing, as well as a comfortable fabric sensor to prevent skin irritation for long-term monitoring [26].

An SSD can be composed of a single sensor or a combination of sensors with certain types of sweat collection devices to perform sweat analysis. A single sensor in an SSD is designed for direct skin contact to detect and measure sweat biomarkers such as metabolites that quickly degrade over time [27]. Thus, adopting a sweat collector, particularly a serpentine microfluidic device for analyzing proteins, is undesirable because sweat flow into a microchannel is time-consuming [28]. However, a sensor that has direct contact with the skin can irritate due to a rough sensor surface and contamination by perspiration from nearby areas. Combining a sensor with certain types of sweat collection devices can overcome these limitations. For example, utilizing paper-microfluidic integration with a sensor can prevent skin inflammation and contamination [29]. Moreover, the addition of paper to a microfluidic device is able to increase the flow rate of the transportation of sweat analytes into a sensor surface by absorption [30]. Therefore, sweat collection devices are essential components that can be added to an SSD. In addition, human sweat glands have small duct diameters, which are 5–40 μm for secretory coils and 10–20 μm for dermal ducts and upper coiled ducts [31], that limit the volume of sweat secretion. As a result, a sweat duct secretes a tiny portion of sweat from the bottom duct into the upper coiled duct region, with a microliter volume of total sweat being released at the skin's surface.

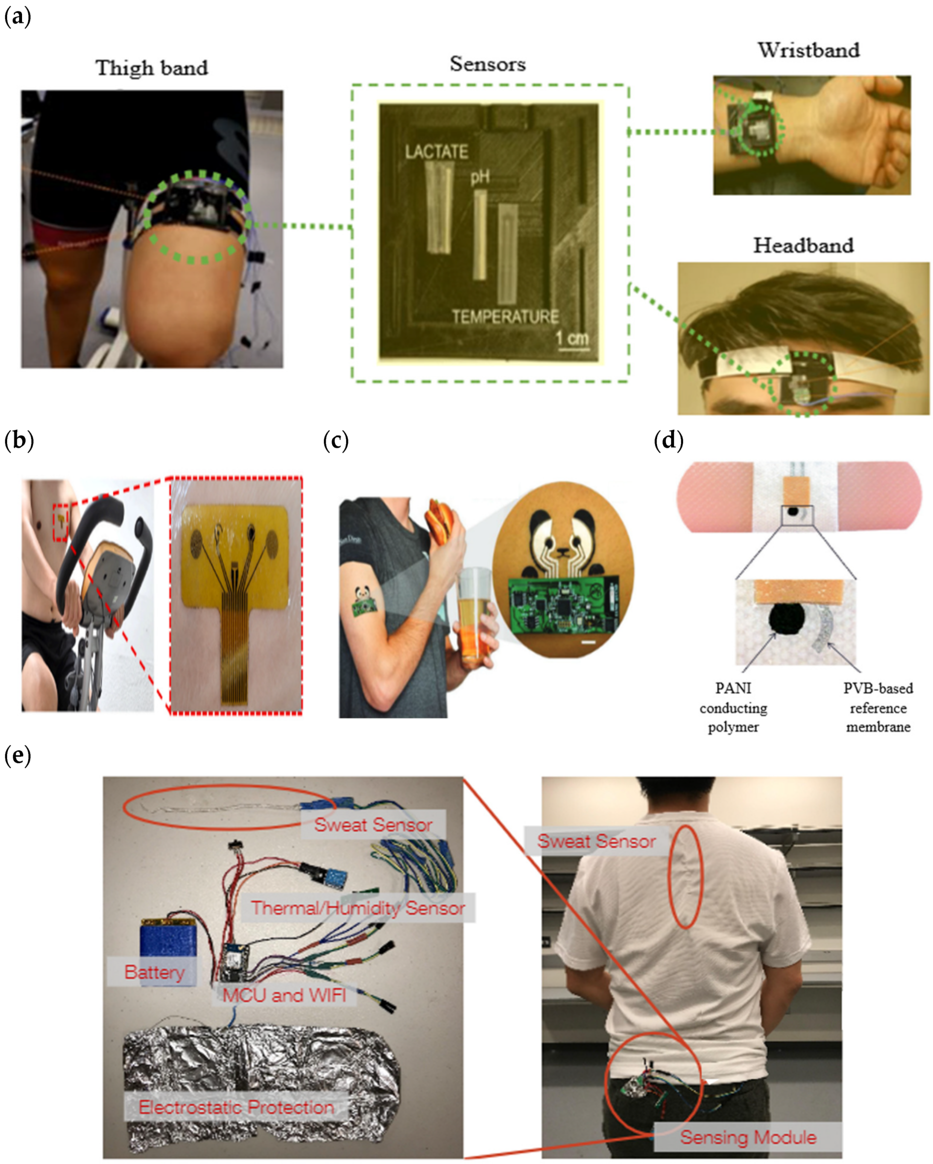

Figure 1. Types of wearable devices in sweat-sensing devices. (**a**) Sweatband [32]; (**b**) skin patch; reprinted from [11], copyright (2022), with permission from Elsevier. (**c**) Tattoo patch [13]; (**d**) bandage of epidermal patch [33] (Reused with the permission of copyright 2014, John Wiley, and Sons). (**e**) Textile [21].

A microfluidic device basically has a channel dimension of tens to hundreds of micrometers to reduce sample consumption and miniaturize microscale instruments for portability [34]. It largely uses body fluid samples such as sweat for the point-of-care diagnosis of diseases and certain laboratory tests. A microfluidic device can be sorted into the mechanism of active micropumps [35][36] and passive micropumps [37][38][39][40][41]. An active micropump requires an external power source to guide a continuous fluid flow with an adjustable flow rate into a microchannel. Typically, an electronic pump is used to deliver a solution efficiently with a setup of a steady flow rate at an inlet cavity that is similar to the natural average velocity [35], pressure, and mass flow rates of a biofluid. It is mainly used to enhance the smooth movement of liquid in a hydrophobic based material channel. Hydrophobic surface will increase resistance of capillary action to the fluid flow during passive flow. Its low surface energy makes it hard to wet on the wall surface, resulting in time-consuming sweat collection on a sensor surface [42].

The combination of a microfluidic device, absorbent-based materials, and microneedle injection demonstrates the best improvements in sweat collection devices, which has a high potential for efficiently transporting a solution in a short time while sharing its combined advantages and overcoming each other's limitations. **Figure 2** shows a summary of various SSD structures, including the types of wearable devices, categories of sweat collection devices, and sweat-sensing devices. There are two main groups for classifying sweat-sensing devices: continuous flow (CF) and non-continuous flow (NCF), based on the presence or absence of an integrated device outlet and real-time measurement. A microfluidic device consists of an outlet, allowing fresh sweat to continuously pass through a sensing area, providing the capability of performing continuous real-time analysis [43][44]. Real-time computation is essential for evaluating precise and valid current sweat analyte concentration withdrawal at a particular time, especially for sweat analysis over a longer period of time [16]. A sensor is commonly used to measure target sweat analytes in real time. CF and NCF SSDs can also be varied in terms of the types of wearable devices and sweat collection devices.

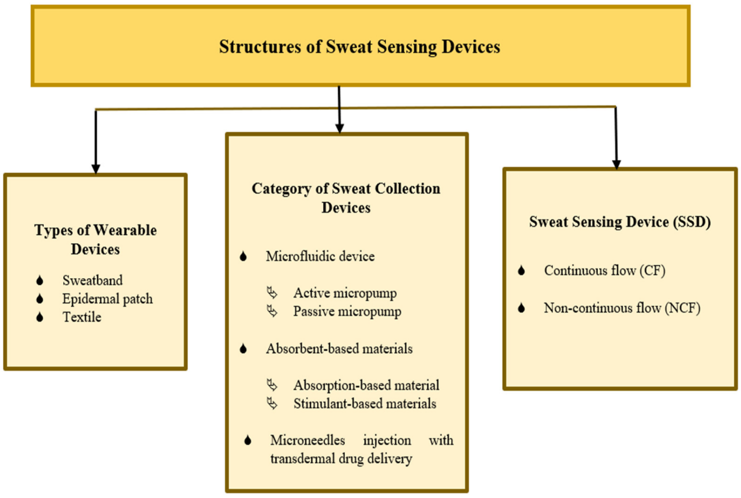

Figure 2. Summary of sweat-sensing device structures.

2. Recent Advances of SSDs: Optimal in Designs, Functionalities, and Performance

2.1. Sweat Collection Device

Adopting pharmacologic agents of sweat-stimulation such as hydrogel and pilocarpine can induce the skin to generate local sweat without requiring physical activity. The iontophoresis of pilocarpine can produce a sufficiently small amount of perspiration within the range of 15–100 µL [45]. Typically, the minimum volume capacity that a chemical sensor can react to and measure is at least 10 to 100 microliters [46]. In addition, this sweat stimulation can also be used to increase the biofluid for an individual that produces a low volume of sweat secretion during exercise. Moreover, the average sweat rate is approximately 1–15 µL min−1 during active secretion [47][48], which slows fluid generation. Therefore, the use of pilocarpine/hydrogel is advocated for stimulating eccrine glands to elevate perspiration levels quickly for exercise and rest. However, most conventional pilocarpine iontophoresis methods are commonly utilized separate processes for collecting sweat samples that are inapplicable outside of the laboratory. Moreover, this process exposes electrical power that can cause skin burning, relying on expensive laboratory equipment and both bulky electrodes and benchtop analyzers [6][9]. Thus, adding a sensor while using this method can provide the dynamic real-time monitoring of target biomarkers on the spot. Kim et al.

developed an SSD that can simultaneously implement the iontophoresis of pilocarpine and the real-time measurement of the continuous monitoring of sweat glucose and alcohol [13].

Employing multiple sweat collection devices in a single SSD can efficiently accumulate a sufficient volume of sweat in a short duration and is able to provide fast hydration monitoring. Gunatilake et al. demonstrated a signal detection time readout of 4 min for lactate and 6 min for glucose using microfluidic paper-based analytical devices by incorporating a hydrogel of alginate-based materials and a colorimetric biosensor [49]. In addition, Alizadeh took 7–10 min for a hydration monitoring application using hydrogel that induced more sweat secretion while utilizing hydrophilic glass wicking in a microfluidic device [50]. In contrast, Nyein et al. only applied a single sweat collector in a microfluidic device which took 30–45 min [36]. However, the period for fitness performance analysis does not mostly depend on the number of sweat collection devices used because it can be flexible when continuously measuring at the user’s preferred target time for estimating the loss of the electrolyte composition. The assembly of various sweat collection tools is primarily concentrated on supporting and maximizing the functions of each other. Incorporating a microfluidic device can hinder the problem of contamination, fast evaporation that reduces the sample collection, and an inevitable blend of renewal sweat concentration [51][52]. In addition, the introduction of a hydrophilic channel can promote capillary pressure, wall adhesion, and hydrostatic forces for the sweat flowing optimally in and out of the chamber. Ideally, a paper-based microfluidic patch could be a viable option to eliminate the direct contact with sensors that causes abrasion, avoid blocking the breathability of glands on the skin, and avoid backflow by increasing the pressure at the inlet during long-time monitoring [53]. Moreover, it facilitates continuous flow collection by transporting the sweat composition in liquid-filled paper channels, and it can also reduce the mixing of old and new sweat [54].

Microneedle transdermal injections can introduce new microbiomes from the surroundings into the skin’s micropores. Although research has demonstrated that skin barrier function can recover the micropores within a few hours [55], utilizing wearable microneedles increases the risk of infection because bacteria can circulate through open micropores on the skin [56]. Moreover, hollow microneedles may fail and shatter due to additional compression, shear stress, excessive motion, the inherent discrepancy in complexion, or any other related pressures [57]. So, standard operating protocols for the use of microneedles are necessary for implementing proper clinical practice. Several mechanical and biological factors of evaluation approaches could be performed in vitro and in vivo to precisely assess possible risks and examine the safety of skin contact with innovative devices, especially when microneedles are used [58][59].

The repeatability of a microfluidic device is vital to ensure it can be frequently reusable, more practicable, prevent the waste of equipment, and avoid relying on disposable products even if they are the cheapest. Yang et al. introduced a reusable microfluidic device that integrated a high selectivity of concurrently detecting lactate and uric acid [60]. Their microfluidic device is portable, small in size, and has lower sample consumption, showing a good design for application prospects in clinical testing and personalized healthcare. Another study developed a microfluidic device that can be repeatedly reused by requiring its chips to be flushed with deionized water to remove the previous biofluid-measured ionic background [61]. Their microfluidic device collects the sweat volume with a small depth size to reduce time-consuming fluid flow. Their wearable microfluidic device is integrated with optimally modified sodium sensors that can measure several applications, such as fitness performance and diagnose cystic fibrosis.

Adding multiple inlet openings to a microfluidic device increases the exposed skin region that releases sweat into the channels while reducing time-consuming sweat secretion that depends on the accumulation in one hole. Xu et al. designed a microfluidic device consisting of eight inlets to reach a reservoir channel at the surface contact of a uric acid electrode sensing interface through the capillary effect [47]. During off-body test, they tested the performance of the microfluidic device by inserting a dye solution with a flow rate of 15 μL min−1 at the inlet. The time required to fill the microfluidic reservoir completely was 166 s. They switched the concentration of the solution between 0–80 μM with a flow rate of 15 μL min−1, while the well-mixed renewal sweat could be used to determine the renewal time, which came out at 4.68 min. Meanwhile, adding multiple outlet openings in a microchannel could also improve passive pump performance through the spontaneous evaporation effect. Cheng et al. developed a wearable sweat sensor consisting of three micropores of the outlet with an inlet cavity [35]. The old sweat solution was quickly transported out by the fluid filling induced by capillary force and followed the spontaneous evaporation effect of micropores at three outlet cavities.

A simulation must be conducted for the fluid flow rate in a microfluidic device before developing its prototype. This is to determine the future channel size and what material properties of the wall are used to provide sufficient pressure without applying external energy. Moreover, a fluid simulation can also be used to mimic a real experiment for the validation of the channel performance of a microfluidic device by defining the average velocity of biological sweat secretion at the inlet. In the experiment, a flow rate sensor must be integrated with a microfluidic device to accurately measure the fluid flow rate. A high correspondence of a good flow rate and short-time results between the fluid simulation and experimental results exhibit the best verification of the effective working of microfluidic device channels. Nyein et al. [36] and the iGEM teams [44] realized both tests, varying the flow rates and solution concentrations. Hence, they had the advantage of exploring and gaining more information about the performance and capability of their device through a variety of changing channel sizes, shapes, and materials via theoretical simulation while saving time and money.

Table 1 shows other more recently developed SSDs with some features related to sweat collection device design. Most of them are CF SSDs that are integrated with sensors for real-time measurement and consist of an outlet in a microfluidic device. In addition, their developed microfluidic device promotes repeatability even though the wearable device is a single-use, disposable epidermal patch. This patch could be replaced with a new patch to allow the sweat collection device to be reused. Moreover, several of them incorporated microchannels with three, six, and eight inlets. Suction pumps and valves were also added to their microfluidic systems to control and increase fluid flow movement. Furthermore, the proposed microfluidic device's validation method was tested, including at least off-body test (calibration) and on-body tests to compare both evaluation performances. In addition, a few of them included a simulation to test the mechanical performance [62][63] as well as the performance in terms of fluid flow [64][65]. Mechanical testing is required to establish the level of flexibility and robustness of the microfluidic device in terms of bending, stretching, and twisting to identify which types of extreme activities they are appropriate for use in. For textile SSDs, it is essential to undergo a process of cleaning and drying for reusability. However, its design should be unaffected by the process, allowing it to retain its functionality.

Table 1. A summary of the latest SSDs' sweat collection device features advancements in 2022.

Categories of Sweat Collection Devices	SSD	Wearable Devices	Dimensions/Depth of Channel	Flow Rate and Time to Fill Channel	Reusable/Disposable	Additional Features	Validation Method	Mechanical Testing	References
Microfluidic device, portable iontophoresis of pilocarpine, adding hydrogel	CF	Epidermal patch	5 mm (Outer diameter), 1 mm (Inner diameter)	N/A 15 min (Total volume 32 μL)	Reusability	Multiple inlets (n = 3)	On-body test	Bending, stretching, twisting	[62]

Categories of Sweat Collection Devices	SSD	Wearable Devices	Dimensions/Depth of Channel	Flow Rate and Time to Fill Channel	Reusable/Disposable	Additional Features	Validation Method	Mechanical Testing	References
Modification of hydrophobic microfluidic device to a hydrophilic surface	CF	Epidermal patch	10 mm (diameter), 1 mm (thickness)	0.05–0.5 m/s (Total volume 200µL)	Reusability	Tesla valves	Simulation, off-body test, on-body test	N/A	[66]
Microfluidic device	CF	Epidermal patch	N/A	3–12 mm/s 13 min for indoor exercise, 20 min for outdoor exercise	Reusability	Multiple inlets (n = 3)	Off-body test, on-body test	Bending, stretching, twisting, tensile	[63]
Modification of hydrophobic microfluidic device to a hydrophilic surface	CF	Epidermal patch	1.5 mm (Inlet diameter), 4 mm (Reservoir diameter), 200 µm (thickness)	0.14 µL/min (each inlet), 0.84 µL/min (total) 14 min (Total volume 11.8 µL)	N/A	Multiple inlets (n = 6)	Simulation, off-body test, on-body test	Bending, pressing	[64]
Microfluidic device	CF	Epidermal patch	1 mm (diameter), 330 µm (thickness)	174.6 µL/min (Total volume 20µL)	N/A	Capillary bursting valves, colorimetric, multiple inlets (n = 8)	Simulation, off-body test, on-body test	Bending, stretching, twisting	[65]
Microfluidic device, absorptive pad	CF	Epidermal patch	N/A	5 µL/min (Total volume 10µL)	Reusability	Suction pump reset after filling the channel	Off-body test, on-body test	N/A	[67]
Textile	NCF	Stitched fabric with three button joints	N/A	N/A	Reusability	Washability	On-body test	Washing, drying (thermal)	[68]

2.2. Sensor

...able Platform for

2. He, W.; Wang, C.; Wang, H.; Jian, M.; Lu, W.; Liang, X.; Zhang, X.; Yang, F.; Zhang, Y. Integrated textile sensor patch for real-time and multiplex sweat analysis. Sci. Adv. 2019, 5, eaax0649.

3. Mostafalu, P.; Akbari, M.; Alberti, K.A.; Xu, Q.; Khademhosseini, A.; Sonkusale, S.R. A toolkit of thread-based microfluidics, sensors, and electronics for 3D tissue embedding for medical diagnostics. Microsyst. Nanoeng. 2016, 2, 16039.

4. Khemtonglang, K.; Chaiyaphet, N.; Kumsaen, T.; Chaiyachati, C.; Chuchuen, O. A Smart Wristband Integrated with an IoT-Based Alarming System for Real-Time Sweat Alcohol Monitoring. Sensors 2022, 22, 6435.

5. Pirovano, P.; Dorrian, M.; Shinde, A.; Donohoe, A.; Brady, A.J.; Moyna, N.M.; Wallace, G.; Diamond, D.; McCaul, M. A wearable sensor for the detection of sodium and potassium in human sweat during exercise. Talanta 2020, 219, 121145.

6. Schazmann, B.; Morris, D.; Slater, C.; Beirne, S.; Fay, C.; Reuveny, R.; Moyna, N.; Diamond, D. A wearable electrochemical sensor for the real-time measurement of sweat sodium concentration. Anal. Methods 2010,

Maintaining a high level of stability in measurement while continuously monitoring a sensor's reliability is challenging. In addition, a high degree of contact between an SSD and the skin can create noise artifacts caused by underlying skin strain or movement. Thus, a great resiliency and robustness of the sensor during extreme physical exercise are essential to enhance the reliability of sweat measurement with minimized dynamic motion artifacts [69]. These mechanical characteristics can maintain a good stability of the sensor's potential, current, or impedance of readable signals for prolonged monitoring even in fluctuating ion concentrations of analytes. The optimization of a surface electrode with polyurethane [70][71], carbon nanotubes [72][73][74], Nafion [73][75], or Ecoflex [76][77] on the solid-contact coating has commonly maintained the contact of electrical conductivity and further high resistance to mechanical stress to ensure strong adherence to conventional substrates. Furthermore, these materials' properties generally include metallic conductivity, high tensile strength, high elasticity, thermal stability, high chemical inertness, and small sizes that are favorable for electrochemical sensor performance [78]. Moreover, with improved solid contact membrane features of electrode sensors based on these materials, the energy generated from mechanical strain can be absorbed, rearranged, and accommodated without deforming, debonding, fracturing, or distorting the electrodes, showing a significant advantage [79]. Hence, the use of modified chemical sensors on the surface of electrodes is essential for long-term measurement, high durability, and stability during extreme movement conditions of physical exercise on an SSD. In the meantime, these fabricated materials can minimize any skin inflammation, fouling, and other adverse physiological effects.

Recently, current state-of-the-art sweat sensor electrodes have frequently been generated from SC-ISEs. Two layers are required: a solid-contact (SC) layer and an ion-selective membrane (ISM). Specifically, the SC layer acts as an ion-to-electron transducer, while the ISM layer acts as an ion recognizer. Introducing material for coating a solid-contact (SC) layer on the first layer before applying an ion-selective membrane (ISM) to the surface of the working electrode (WE) and reference electrode (RE) can also improve a sensor's sensitivity to detect a specific analyte. The materials most often used in SC layers are poly-3,4-ethylenedioxythiophene (PEDOT) [36][80][81], polyaniline (PANI) [82], Prussian-Blue (PB) [83], Chitosan/Prussian Blue Nanocomposite (ChPBN) [84], and Poly(vinyl acetate)/inorganic salts (PVA/KCl) [7], poly(3-octylthiophene) (POT) [85]. These materials have exhibited the promising features of good sensitivity, high selectivity, and consistent stability in terms of the measurement of electrochemical sensors. PEDOT is a popular SC layer that has frequently been coated on electrode sensors and can be utilized to detect a wide range of sweat biomarkers. PEDOT can be made more effective and more diverse by mixing it with various chemicals such as the synthesis of PEDOT/PB, PEDOT/KCl, PEDOT(1-Ethyl-3-methylimidazoliumbis(trifluoromethylsulfonyl)imide) as PEDOT[emim][NTf2]), PEDOT(1-ethyl-3-methylimidazolium tris(pentafluoroethyl) trifluorophosphate) as PEDOT[emim][FAP]), and PEDOT Polystyrene Sulfonate (PEDOT/PSS). Matzeu et al. tested the performance of four different chemical solutions of PEDOT, namely as PEDOT(KCl), PEDOT[emim][FAP], PEDOT[emim][NTf2], and PEDOT/PB in detecting sodium ions [61]. All the PEDOT SC-layers that they grew showed an average sensitivity of slopes near the sub-Nernstian of the calibration slope within a concentration range of 10−4–10−1 M. They showed that PEDOT[emim][NTf2]) was the best PEDOT SC-layer because of its smallest significance in the standard deviation for the calibration curves of the slope's offset sensitivity. This SC layer material could give good repeatability and a long life span within 5 weeks, according to Alizadeh et al. [50], and 6 weeks, according to Zuliani et al. [85]. A modified electrode surface with a solid-contact layer of PEDOT/PSS membrane could also give long-term repeatability and stable responses at various physiological temperatures [86]. Wei Gao et al. developed a sodium sensor with reproducibility and long-term stability for at least four weeks by incorporating an SC layer of a PEDOT/PSS membrane on the WE and a CNT membrane on the RE [87].

Particularly, PANI coating has been applied in pH sensors to optimize the analytical performance, including good repeatability and a sensitivity range for pH measurement between 4 and 7 to detect acidic sweat [88][89]. Meanwhile, PB and chitosan are widely used in the fabrication of glucose and lactate sensors, according to a few studies [90][91]. Bandodkar et al. reported that

2, 342–348.
7. Wang, S.; Wu, Y.; Gu, Y.; Li, T.; Luo, H.; Li, L.H.; Bai, Y.; Li, L.; Liu, L.; Cao, Y.; et al. Wearable Sweatband Sensor Platform Based on Gold Nanodendrite Array as Efficient Solid Contact of Ion-Selective Electrode. Anal. Chem. 2017, 89, 10224–10231.
8. Gonzalo-Ruiz, J.; Mas, R.; de Haro, C.; Cabruja, E.; Camero, R.; Alonso-Lomillo, M.A.; Muñoz, F.J. Early determination of cystic fibrosis by electrochemical chloride quantification in sweat. Biosens. Bioelectron. 2009, 24, 1788–1791.
9. Choi, J.; Ghaffari, R.; Baker, L.B.; Rogers, J.A. Skin-interfaced systems for sweat collection and analytics. Sci. Adv. 2018, 4, eaar3921.
10. McLister, A.; McHugh, J.; Cundell, J.; Davis, J. New Developments in Smart Bandage Technologies for Wound Diagnostics. Adv. Mater. 2016, 28, 5732–5737.
11. Yoon, S.; Yoon, H.; Zahed, M.A.; Park, C.; Kim, D.; Park, J.Y. Multifunctional hybrid skin patch for wearable smart healthcare applications. Biosens. Bioelectron. 2022, 196, 113685.
12. Bandodkar, A.J.; Molinnus, D.; Mirza, O.; Guinovart, T.; Windmiller, J.R.; Valdés-Ramírez, G.; Andrade, F.J.; Schöning, M.J.; Wang, J. Epidermal tattoo potentiometric sodium sensors with wireless signal transduction for continuous non-invasive sweat monitoring. Biosens. Bioelectron. 2014, 54, 603–609.
13. Kim, J.; Sempionatto, J.R.; Imani, S.; Hartel, M.C.; Barfidokht, A.; Tang, G.; Campbell, A.S.; Mercier, P.P.; Wang, J.; Kim, J.; et al. Simultaneous Monitoring of Sweat and Interstitial Fluid Using a Single Wearable Biosensor Platform. Adv. Sci. 2018, 5, 1800880.
14. Terse-Thakoor, T.; Punjiya, M.; Matharu, Z.; Lyu, B.; Ahmad, M.; Giles, G.E.; Owyeung, R.; Alaimo, F.; Shojaei Baghini, M.; Brunyé, T.T.; et al. Thread-based multiplexed sensor patch for real-time sweat monitoring. Npj Flex. Electron. 2020, 4, 18.
15. Jiang, X.; Lillehoj, P.B. Microneedle-based skin patch for blood-free rapid diagnostic testing. Microsyst. Nanoeng. 2020, 6, 96.
16. Seshadri, D.R.; Li, R.T.; Voos, J.E.; Rowbottom, J.R.; Alfes, C.M.; Zorman, C.A.; Drummond, C.K. Wearable sensors for monitoring the physiological and biochemical profile of the athlete. Npj Digit. Med. 2019, 2, 72.
17. Reeder, J.T.; Choi, J.; Xue, Y.; Gutruf, P.; Hanson, J.; Liu, M.; Ray, T.; Bandodkar, A.J.; Avila, R.; Xia, W.; et al. Waterproof, electronics-enabled, epidermal microfluidic devices for sweat collection, biomarker analysis, and thermography in aquatic settings. Sci. Adv. 2019, 5, eaau6356.
18. Wang, L.; Xu, T.; He, X.; Zhang, X. Flexible, self-healable, adhesive and wearable hydrogel patch for colorimetric sweat detection. J. Mater. Chem. C 2021, 9, 14938–14945.
19. Kim, J.; Wu, Y.; Luan, H.; Yang, D.S.; Cho, D.; Kwak, S.S.; Liu, S.; Ryu, H.; Ghaffari, R.; Rogers, J.A.; et al. A Skin-Interfaced, Miniaturized Microfluidic Analysis and Delivery System for Colorimetric Measurements of Nutrients in Sweat and Supply of Vitamins Through the Skin. Adv. Sci. 2021, 9, 2103331.
20. Wicaksono, I.; Tucker, C.I.; Sun, T.; Guerrero, C.A.; Liu, C.; Woo, W.M.; Pence, E.J.; Dagdeviren, C. A tailored, electronic textile conformable suit for large-scale spatiotemporal physiological sensing in vivo. Npj Flex. Electron. 2020, 4, 5.

their epidermal tattoo demonstrated an excellent high-detection potential in sweat glucose when the nanotextile was modified with Prussian Blue, which exhibited a better performance compared to GlucoWatch, which could lead to compromised selectivity [83]. Moreover, PB is a redox molecule commonly used to modify electrodes to increase the upper detection limit of lactate sensors [92][93][94]. In addition, combining several SC layers, such as ChPBN, can provide a wide range of detection for target sweat biomarkers. As an example, Tanusree et al. detected the presence of sodium ions with good potential sensitivity that a near-Nernstian response of 58 mV for sodium in a wide linear range, i.e., 10−7−1 M in a sodium phosphate buffer (NaPB) [84]. Furthermore, their modified electrode provided an excellent stability response with the smallest potential drift of 3.61 × 10^{-4} μV/s, showing a small to almost negligible potential drift, stabilizing the abnormal potential response and increasing the life span effectiveness. Furthermore, the highly porous structure of the ChPBN layer provided a high interfacial area that enhanced the effectiveness of the ion sensing and induced greater selectivity (103–104 times higher) towards sodium ions. In summary, most of the proposed SC layer materials used for modifying the ISE sensor surface have promoted good stability and repeatability for long-term use. As a result, there was no ionophore leaking from the ISE into the solution; thus, good sensitivity and selectivity were maintained when the SC layer was introduced. This was because ISM components have a lower solubility due to their improved lipophilicity. This SC also provided more resistance to biofouling, which is advantageous for practical measurements at high concentrations.

Most ISEs with antibiotic ionophore coatings provide high target biomarker selectivity. For instance, valinomycin ISE has an inherent permeability specific to the recognition of potassium ions, allowing the membrane to detect them selectively [76][95]. However, valinomycin contains biological toxicity that has been often ignored and could be a daunting challenge. A potassium-ion lattice intercalation (PILI) [96][97][98] can be used to replace valinomycin to solve this problem. This is because PILI can potentially form SC-ISE-based battery materials without the need for an ISM coating for sensing potassium ions potentiometrically. PILI can also serve as SC-ISEs with a single-piece structure that is already present with directly mixed SC and ISM for ion-response realization. Thus, this SC layer is capable of both ion recognition and ion-to-electron transduction functions. Moreover, it can prevent the creation of a water layer at the SC/ISM phase boundary as well as prevent the leaking of ISM components, both of which are caused by the ISM. This concept comes from the SC-ISE based on Li-ion battery materials as an SC layer without the use of ISM, wherein the proposed lithium manganese oxide (LiMn2O4) electrode exhibits a Nernstian response toward lithium-ion sensing in human blood serum solution [99]. Their study highlighted non-ISM-based SC-ISEs for potentiometric ion sensing, which displayed a comparable sensitivity, selectivity, stability, and linear range to conventional SC-ISEs incorporating ISMs.

Utilizing optical sensing in SSDs enables the provision of a light-delivery indicator for the easy visualization and analysis of present particular sweat biomarkers with the naked eye. Colorimetric sensors [52] and fluorescent sensors [100] are the forms of optical sensing most found in recent SSDs. Kim et al. reported a soft, thin colorimetric patch mounted with a microfluidic device that consists of passive valving [19]. Flowing sweat in their colorimetry sensing channel changed the color indicators depending on the loss of iron, zinc, calcium, and vitamin C nutrients. Their device then triggered the delivery of similar amounts of these nutrients with blood transdermally after the sweat secretion filled the depths of a micro-reservoir channel. Most colorimetric sensing applies a simple design without a required electronic device, wireless communication, soft, flexible strength, thin structure, and non-irritating interaction with the epidermis [17][101]. In particular, optical sensors encapsulate specific reagents to produce measurable changes in the optical wavelength for visual information when reacting with the target sweat biomarker. For example, the chemical reaction and absorbance of sweat analyte concentrations by reagent substances in a colorimetric sensor can change color when presenting a specific biomarker [102]. Meanwhile, a fluorescent sensor contains an active chemical fluorescent dye to detect the presence of target analyte concentration changes by responding to a fluorescence intensity change [103]. This sensing method uses optical modules containing LEDs, filters, and a camera to make visible fluorescent probes that detect biomarker concentrations [100].

21. Jia, J.; Xu, C.; Pan, S.; Xia, S.; Wei, P.; Noh, H.Y.; Zhang, P.; Jiang, X. Conductive Thread-Based Textile Sensor for Continuous Perspiration Level Monitoring. Sensors 2018, 18, 3775.

22. Someya, T.; Amagai, M. Toward a new generation of smart skins. Nat. Biotechnol. 2019, 37, 382–388.

23. Majumder, S.; Mondal, T.; Deen, M.J. Wearable Sensors for Remote Health Monitoring. Sensors 2017, 17, 130.

24. Cancela, J.; Pastorino, M.; Tzallas, A.T.; Tsipouras, M.G.; Rigas, G.; Arredondo, M.T.; Fotiadis, D.I. Wearability Assessment of a Wearable System for Parkinson's Disease Remote Monitoring Based on a Body Area Network of Sensors. Sensors 2014, 14, 17235–17255.

25. Martinez-Estrada, M.; Moradi, B.; Fernández-Garcia, R.; Gil, I. Impact of Manufacturing Variability and Washing on Embroidery Textile Sensors. Sensors 2018, 18, 3824.

26. Koo, H.; Hebrio, I.; Johnston, M.; Hosein, N.; Fallon, K. StressSense: Skin conductivity monitoring garment with a mobile app. In Proceedings of the 2016 ACM International Joint Conference on Pervasive and Ubiquitous Computing: Adjunct, Heidelberg, Germany, 12–16 September 2016; pp. 487–490.

27. Peterson, R.A.; Gueniche, A.; De Beaumais, S.A.; Breton, L.; Dalko-Csiba, M.; Packer, N.H. Sweating the small stuff: Glycoproteins in human sweat and their unexplored potential for microbial adhesion. Glycobiology 2016, 26, 218–229.

28. Brett, M.E.; Zhao, S.; Stoia, J.L.; Eddington, D.T. Controlling flow in microfluidic channels with a manually actuated pin valve. Biomed. Microdevices 2011, 13, 633–639.

29. Mogera, U.; Guo, H.; Namkoong, M.; Rahman, M.S.; Nguyen, T.; Tian, L. Wearable plasmonic paper–based microfluidics for continuous sweat analysis. Sci. Adv. 2022, 8, 1736.

30. Abbasiasl, T.; Mirlou, F.; Istif, E.; Koydemir, H.C.; Beker, L. A wearable paper-integrated microfluidic device for sequential analysis of sweat based on capillary action. Sens. Diagn. 2022, 1, 775–786.

31. Sonner, Z.; Wilder, E.; Heikenfeld, J.; Kasting, G.; Beyette, F.; Swaile, D.; Sherman, F.; Joyce, J.; Hagen, J.; Kelley-Loughnane, N.; et al. The microfluidics of the eccrine sweat gland, including biomarker partitioning, transport, and biosensing implications. Biomicrofluidics 2015, 9, 031301.

32. Xuan, X.; Pérez-Ràfols, C.; Chen, C.; Cuartero, M.; Crespo, G.A. Lactate Biosensing for Reliable On-Body Sweat Analysis. ACS Sens. 2021, 6, 2763–2771.

33. Guinovart, T.; Valdés-Ramírez, G.; Windmiller, J.R.; Andrade, F.J.; Wang, J. Bandage-Based Wearable Potentiometric Sensor for Monitoring Wound pH. Electroanalysis 2014, 26, 1345–1353.

34. Park, J.W.; Vahidi, B.; Taylor, A.M.; Rhee, S.W.; Jeon, N.L. Microfluidic culture platform for neuroscience research. Nat. Protoc. 2006, 1, 2128–2136.

35. Chen, X.M.; Li, Y.J.; Han, D.; Zhu, H.C.; Xue, C.D.; Chui, H.C.; Cao, T.; Qin, K.R. A capillary-evaporation micropump for real-time sweat rate monitoring with an electrochemical sensor. Micromachines 2019, 10, 457.

36. Nyein, H.Y.Y.; Tai, L.C.; Ngo, Q.P.; Chao, M.; Zhang, G.B.; Gao, W.; Bariya, M.; Bullock, J.; Kim, H.; Fahad, H.M.; et al. A Wearable Microfluidic Sensing Patch for Dynamic Sweat Secretion Analysis. ACS Sens. 2018, 3, 944–952.

Recently, wearable sweat optical sensors that function with a smartphone to benefit from technology by capturing and processing images, data analysis, data transfer, data storage, and cloud software systems have been developed [104]. Ardalan et al. developed an epidermal patch with fluorescent sensing based on a smartphone that included the multi-sensing of a wide range of sweat biomarkers in real time, including sweat rate, glucose, lactate, chloride, and pH [105]. In their studies, paper discs with fluorogenic reagents were equipped as sensors, threads in the microchannels retrieved the sweat fluid and conveyed it to the paper sensor, and transparent medical-grade adhesives were used to keep the substrates (paper and thread) in contact with the skin. In brief, an optical sensing device is more appropriate for measuring pH because the results reflect color-changing that is easily observed in color indicator analysis and for multiple analyte measurements that more than three sensors can be integrated [17][52][101][102]. Additionally, this mostly exploits the serpentine channels that store optical assay reagents to increase the surface area of the microfluidic device to store and analyze sweat. In addition, there is no need for a power supply to run the entire system and analyze biomarkers when it is integrated with optical sensing [19].

However, optical sensors perform limited monitoring of sweat sensing in discontinuous flow mode. Thus, adopting an electrochemical sensor into an SSD enables the measuring of target analytes in continuous or discontinuous flow modes. Continuous flow measurement can be set by adding the feature of the outlet channel to a microfluidic device with the integration of a chemical sensor, while discontinuous measurement is the opposite of this design. Discontinuous flow measurement involves the conventional iontophoresis test (Macroduct® system), which is implemented in a separate procedure from sweat stimulation, sample collection, and sweat analyzing. Moreover, an electrochemical sensor has a transducer to detect the target analyte concentration in sweat and convert this chemical reaction into a readable electrical signal (current/voltage/impedance) for amplification and data processing [106]. Amplification is required to increase the readability of the original signal state for such a small concentration unit of the electrochemical signal. The concentration of analytes in sweat is too small, it being in millimolar [107] and micromolar units. The analyzing of readable signals of analytes present in various concentrations of dynamic sweat in real time can be implemented using the electrochemical signal measurement technique. Electrochemical impedance spectroscopy (EIS) [84][108], potentiometric [77][81], and cyclic voltammetry (CV) [109][110] are widely applied techniques in detecting and computing analytes in sweat using electrochemical sensors. Before being performed in sweat analysis on the body, an electrochemical sensor requires a validation and calibration test to establish a reliable electrode. However, an optical sensor can only be used once, which can simply direct measurement without the need for calibration. Furthermore, an electrochemical sensor can also capture and transmit data digitally by wireless wearable electrochemical sensors that track the metabolic activity and physiological state with great resolution in remote areas [111]. In brief, electrochemical sensing relies on the electrochemical signal measurement technique in evaluating analyte perspiration; this sensor is suitable for applications needing large data for continuous measurement and measuring several analytes, with the electrode fabrication not exceeding three sensors. In addition, optical and electrochemical sensing can be combined to optimize the functioning of sensors. Kim et al. used hybrid colorimetric and electrochemical sensing integrated with a microfluidic device to provide the multimodal analysis of sweat glucose, lactate, chloride, pH, and sweat rate [101]. Remarkably, it realized visual and excitation light delivery with a detailed readable signal via the amperometry method.

Even when analyzing a single sweat application, integrating multiple sensors is needed to add important information, deeply understand the analyte reactions, and precisely analyze the disease conditions. For example, in kidney diagnosis, urea and creatinine sensors are used to diagnose kidney disease in sweat, while pH sensors can identify different stages of it chronically [112]. In another practice, the evaluation of calcium concentration requires pH measurement as an indicator of high and low calcium secretion in real time [113]. Sweat pH declines when the lactic acid concentration drops while the calcium concentration increases. On the other hand, the sweat pH is also relevant, coupled with the sodium concentration for monitoring hydration. pH measurement gives individual variability in the reproducible evaluation of sweat sodium

37. Zhu, Y.; Granick, S. Rate-Dependent Slip of Newtonian Liquid at Smooth Surfaces. Phys. Rev. Lett. 2001, 87, 096105.
38. Choi, C.H.; Westin, K.J.A.; Breuer, K.S. Apparent slip flows in hydrophilic and hydrophobic microchannels. Phys. Fluids 2003, 15, 2897.
39. Zhang, Y.; Chen, Y.; Huang, J.; Liu, Y.; Peng, J.; Chen, S.; Song, K.; Ouyang, X.; Cheng, H.; Wang, X. Skin-interfaced microfluidic devices with one-opening chambers and hydrophobic valves for sweat collection and analysis. Lab Chip 2020, 20, 2635–2645.
40. White, T.; Kaya, T. Evaluation of Hydrophilic Properties of Polydimethylsiloxane for Possible Microfluidic Sweat Sensor Applications. 2016. Available online: http://people.se.cmich.edu/yelam1k/asee/proceedings/2016/student_regular_papers/2016_asee_ncs_paper_19.pd (accessed on 26 February 2022).
41. Escobedo, P.; Ramos-Lorente, C.E.; Martínez-Olmos, A.; Carvajal, M.A.; Ortega-Muñoz, M.; de Orbe-Payá, I.; Hernández-Mateo, F.; Santoyo-González, F.; Capitán-Vallvey, L.F.; Palma, A.J.; et al. Wireless wearable wristband for continuous sweat pH monitoring. Sens. Actuators B Chem. 2021, 327, 128948.
42. Design engineer considerations when selecting materials and designing microfluidic devices. Adv. Healthc. Mater. 2018, 6, 1601403.
43. Curto, V.F.; Fay, C.; Coyle, S.; Byrne, R.; O'Toole, C.; Barry, C.; Hughes, S.; Moyna, N.; Diamond, D.; Benito-Lopez, F. Real-time sweat pH monitoring based on a wearable chemical barcode micro-fluidic platform incorporating ionic liquids. Sens. Actuators B Chem. 2012, 171–172, 1327–1334.
44. The International Genetically Engineered Machine (IGEM), Hardware (Microfluidic, Biosensor and Electronic Device) Rochester Team. 2021. Available online: https://2021.igem.org/Team:Rochester/Hardware#here2 (accessed on 26 February 2022).
45. Li, S.; Hart, K.; Norton, N.; Ryan, C.A.; Guglani, L.; Prausnitz, M.R. Administration of pilocarpine by microneedle patch as a novel method for cystic fibrosis sweat testing. Bioeng. Transl. Med. 2021, 6, e10222.
46. Kim, J.; de Araujo, W.R.; Samek, I.A.; Bandodkar, A.J.; Jia, W.; Brunetti, B.; Paixao, T.R.; Wang, J. Wearable temporary tattoo sensor for real-time trace metal monitoring in human sweat. Electrochem. Commun. 2015, 51, 41–45.
47. Xu, Z.; Song, J.; Liu, B.; Lv, S.; Gao, F.; Luo, X.; Wang, P. A conducting polymer PEDOT:PSS hydrogel based wearable sensor for accurate uric acid detection in human sweat. Sens. Actuators B Chem. 2021, 348, 130674.
48. Lin, H.; Tan, J.; Zhu, J.; Lin, S.; Zhao, Y.; Yu, W.; Hojaiji, H.; Wang, B.; Yang, S.; Cheng, X.; et al. A programmable epidermal microfluidic valving system for wearable biofluid management and contextual biomarker analysis. Nat. Commun. 2020, 11, 4405.
49. Gunatilake, U.B.; Garcia-Rey, S.; Ojeda, E.; Basabe-Desmonts, L.; Benito-Lopez, F. TiO2 Nanotubes Alginate Hydrogel Scaffold for Rapid Sensing of Sweat Biomarkers: Lactate and Glucose. ACS Appl. Mater. Interfaces 2021, 13, 37734–37745.

concentration [114]. Occasionally, sodium sensing is customarily hybridized with a potassium sensor [5], thus being vastly exploited for wearable SSDs in sports analysis, which continuously monitor the sweat electrolytes during exercise [72]. The association of multiple electrolyte sensors in a single SSD provides a better fitness performance analysis, which contributes to accurate measurements.

Additionally, an SSD that integrates with various chemical sensors can also be featured in multitasking sweat applications such as medical diagnostics and the analysis of fitness performance, to reduce time consumption by simultaneously analyzing the different purposes of sweat measurement. For instance, Bandodkar et al. developed a sweat multiplexed sensing system that monitors pH, temperature, lactate, glucose, and chloride concentrations to detect changes in the concentration of those biomarkers corresponding with specific fitness conditions and hydration levels [115]. Furthermore, Nyein et al. developed multiplex electrochemical sensors comprising pH, chloride ion, and levodopa composition sensing, which were used to associate with sweat released due to the response of physical and mental stress while the subjects were in a resting position [116]. When at rest, sweating more or less may be an additional sign of autonomic dysfunction, diabetes, cerebrovascular disease, Parkinson's disease, and chronic psychological stress such as anxiety or pain [117][118]. Sweat pH can indicate acid–base imbalances [4], whereas chloride levels are helpful in testing for cystic fibrosis, electrolyte balance, and hydration status [80]. Sweat-based levodopa screening could contribute to precision therapy for Parkinson's patients [119]. They optimally maximized multifunction sweat applications, including physical hydration, neurological afflictions, and mental condition.

In sweat analysis, adding physical/physiological signal sensors (e.g., blood pressure, heart rate, and electrocardiograms) that integrate with a chemical sensor can provide a sufficient overview of a patient's health condition, the body's response, and physiological changes to daily activities. Sempionatto et al. constructed an SSD that could monitor vital signs (blood pressure and heart rate), the concentration of metabolites (glucose and lactate), and exogenous chemical levels (caffeine and alcohol) by analyzing sweat extracted through exercise, iontophoresis, and external stimuli (intake of food, caffeine, and alcohol) [120]. These biomarker sensors were proposed to have a correlation with the health self-monitoring of common daily activities such as eating, drinking, and exercising. Their SSD was optimized to provide good mechanical resilience and a dependable glucose detection in sweat without crosstalk between the different sensors. In addition, Imani et al. proposed an epidermal patch that could continually track sweat lactate levels and ECG signals concurrently to assess a wearer's physical strength, exercise intensity, and tissue oxygenation [121]. It is possible to monitor the health and function of the heart using electrocardiograms, while sweat lactate sensor integration can be used to monitor an individual's fitness performance and diagnose tissue oxygenation and pressure ischemia. This device offers a practical approach to researching and developing multimodal wearable sensors that incorporate physical, electrophysiological, and chemical sensors to further measure human physiology comprehensively.

Table 2 shows the latest developed SSDs with various sensor features and measurements that have previously been discussed, such as solid contact materials, sensor types (electrochemical or colorimetric), and the incorporation of a physical/physiological signal sensor. These features are essential for determining whether the newest SSDs can be used repeatedly over the long term and whether they have already maximized their advanced performance by including multiple sensors, biophysical sensing, and multiple analyte measurement. The life span of the developed sensors was kept stable, with minimal drift of measurement values in current or voltage. In addition, blood testing, together with sweat analysis, can provide a good comparison and evaluate whether both biofluid samples have a strong correlation in order to check the reliability of the created sensor device and the practicability of the sweat sampling analysis for certain biomarkers [11][62].

Sweat has remained comparatively unexplored in comparison to standard biofluids, such as blood, despite its great promise for noninvasive physiological monitoring.

50. Alizadeh, A.; Burns, A.; Lenigk, R.; Gettings, R.; Ashe, J.; Porter, A.; McCaul, M.; Barrett, R.; Diamond, D.; White, P.; et al. A wearable patch for continuous monitoring of sweat electrolytes during exertion. Lab Chip 2018, 18, 2632–2641.
51. Martín, A.; Kim, J.; Kurniawan, J.F.; Sempionatto, J.R.; Moreto, J.R.; Tang, G.; Campbell, A.S.; Shin, A.; Lee, M.Y.; Liu, X.; et al. Epidermal Microfluidic Electrochemical Detection System: Enhanced Sweat Sampling and Metabolite Detection. ACS Sens. 2017, 2, 1860–1868.
52. Choi, J.; Xue, Y.; Xia, W.; Ray, T.R.; Reeder, J.T.; Bandodkar, A.J.; Kang, D.; Xu, S.; Huang, Y.; Rogers, J.A. Soft, skin-mounted microfluidic systems for measuring secretory fluidic pressures generated at the surface of the skin by eccrine sweat glands. Lab Chip 2017, 17, 2572–2580.
53. Liang, B.; Wei, J.; Tu, T.; Cao, Q.; Mao, X.; Fang, L.; Ye, X. A Smartwatch Integrated with a Paper-based Microfluidic Patch for Sweat Electrolytes Monitoring material science View project Two Dimensional Carbon Materials Based Gas Sensor Development View project A Smartwatch Integrated with a Paper-based Microfluidi. Electroanalysis 2020, 33, 643–651.
54. Lan, W.J.; Maxwell, E.J.; Parolo, C.; Bwambok, D.K.; Subramaniam, A.B.; Whitesides, G.M. Paper-based electroanalytical devices with an integrated, stable reference electrode. Lab Chip 2013, 13, 4103–4108.
55. Kalluri, H.; Kolli, C.S.; Banga, A.K. Characterization of microchannels created by metal microneedles: Formation and closure. AAPS J. 2011, 13, 473–481.
56. McConville, A.; Hegarty, C.; Davis, J. Mini-Review: Assessing the Potential Impact of Microneedle Technologies on Home Healthcare Applications. Medicines 2018, 5, 50.
57. Kochhar, J.S.; Soon, W.J.; Choi, J.; Zou, S.; Kang, L. Effect of microneedle geometry and supporting substrate on microneedle array penetration into skin. J. Pharm. Sci. 2013, 102, 4100–4108.
58. Park, J.H.; Allen, M.G.; Prausnitz, M.R. Biodegradable polymer microneedles: Fabrication, mechanics and transdermal drug delivery. J. Control. Release 2005, 104, 51–66.
59. Bal, S.M.; Caussin, J.; Pavel, S.; Bouwstra, J.A. In vivo assessment of safety of microneedle arrays in human skin. Eur. J. Pharm. Sci. 2008, 35, 193–202.
60. Yang, S.; Lu, F.; Liu, Y.; Ning, Y.; Tian, S.; Zuo, P.; Ji, X.; He, Z. Quantum dots-based hydrogel microspheres for visual determination of lactate and simultaneous detection coupled with microfluidic device. Microchem. J. 2021, 171, 106801.
61. Matzeu, G.; O'Quigley, C.; McNamara, E.; Zuliani, C.; Fay, C.; Glennon, T.; Diamond, D. An integrated sensing and wireless communications platform for sensing sodium in sweat. Anal. Methods 2015, 8, 64–71.
62. Bolat, G.; De la Paz, E.; Azeredo, N.F.; Kartolo, M.; Kim, J.; de Loyola e Silva, A.N.; Rueda, R.; Brown, C.; Angnes, L.; Wang, J.; et al. Wearable soft electrochemical microfluidic device integrated with iontophoresis for sweat biosensing. Anal. Bioanal. Chem. 2022, 414, 5411–5421.
63. Wei, J.; Fang, G.; Kuang, Z.; Cheng, L.; Wu, H.; Guo, D.; Liu, A. 3D-printed low-cost fabrication and facile integration of flexible epidermal microfluidics platform. Sens. Actuators B Chem. 2022, 353, 131085.
64. He, X.; Fan, C.; Luo, Y.; Xu, T.; Zhang, X. Flexible microfluidic nanoplasmonic sensors for refreshable and portable recognition of sweat biochemical fingerprint. Npj Flex. Electron. 2022, 6, 60.

65. Liu, S.; Som Yang, D.; Wang, S.; Luan, H.; Sekine, Y.; Model, J.B.; Aranyosi, A.J.; Ghaffari, R.; Rogers, J.A.; John Rogers, C.A.; et al. Soft, environmentally degradable microfluidic devices for measurement of ... 2022, 13,
6... valve-based
6... ey, A. ... 2022, 7, 1156–
6... nart textile
6... -free electronic
7... Multi-Ion
7... , E. A ... an Perspiration.
7... , Y.; Evans, J.W.; ... weat. APL Mater.
7... All-in-one, ... Sens. Actuators

Table 2. A summary of the latest SSDs' sensor features and advancements in 2022.

Analytes Detection	Solid Contact Materials	Types of Sensors	Physical/ Physiological Signal Sensor	Sample	Correlate with Blood Test	Techniques Measurements	Repeatability and Life Span	References
Levodopa	Zeolitic imidazolate framework/ graphene oxide (ZIF-8/GO)	Electrochemical	N/A	Sweat	Yes	Chronoamperometry, cyclic voltammetry	N/A 7 days	[122]
Glucose	PB	Colorimetry, electrochemical	N/A	Sweat, blood	Yes	Amperometry	N/A	[62]
Lactate	N/A	Colorimetric	Temperature	Artificial sweat, human sweat	Yes	Convolutional neural networks (CNNs)	N/A	[123]
Glucose, pH	PANI, reduced glucose oxidase (GOx)/ PtNPs/ Gold (Au)	Electrochemical	ECG, temperature, heart rate	Artificial sweat, human sweat, blood	Yes	Amperometry, potentiometry	Repeatability 1 week	[11]
Cl−, pH	N/A	Colorimetric	N/A	Artificial sweat, human sweat	N/A	Color intensity changing (absorbance, wavelength)	N/A	[65]
Glucose	PB-PEDOT-N	Electrochemical	N/A	Sweat, blood	Yes	Chronoamperometry	Repeatability 1 month	[75]
Na+, K+	PEDOT/PSS	Electrochemical	N/A	Sweat	N/A	Chronoamperometry, potentiometry	Repeatability -	[81]
Na+, K+, pH	PEDOT/PSS, PANI	Electrochemical	N/A	Sweat	N/A	Chronoamperometry, potentiometry	Repeatability 30 days	[124]
Na+, K+,Pb+2,Li+	Platinum nanoparticles (PtNPs)	Electrochemical	Temperature	NaCl, KCl, LiCl, Pb(NO3)2	Yes	Potentiometry	N/A	[125]
Glucose, lactate	PB	Electrochemical	Heart rate	Sweat	Yes	Amperometry	Disposable	[126]
Uric acid	Metal azolate framework-7 (MAF-7)	Electrochemical	N/A	Artificial sweat, human sweat	N/A	Amperometry, cyclic voltammetry	N/A	[127]
Creatinine	N/A	Fluorescence	N/A	Sweat, urine	Yes	Color intensity changing (absorbance, wavelength)	N/A	[128]

74. Yoon, J.H.; Kim, S.M.; Eom, Y.; Koo, J.M.; Cho, H.W.; Lee, T.J.; Lee, K.G.; Park, H.J.; Kim, Y.K.; Yoo, H.J.; et al. Extremely Fast Self-Healable Bio-Based Supramolecular Polymer for Wearable Real-Time Sweat-Monitoring Sensor. ACS Appl. Mater. Interfaces 2019, 11, 46165–46175.
75. Lin, P.H.; Sheu, S.C.; Chen, C.W.; Huang, S.C.; Li, B.R. Wearable hydrogel patch with noninvasive, electrochemical glucose sensor for natural sweat detection. Talanta 2022, 241, 123187.
76. Zhai, Q.; Yap, L.W.; Wang, R.; Gong, S.; Guo, Z.; Liu, Y.; Lyu, Q.; Wang, J.; Simon, G.P.; Cheng, W. Vertically Aligned Gold Nanowires as Stretchable and Wearable Epidermal Ion-Selective Electrode for Noninvasive Multiplexed Sweat Analysis. Anal. Chem. 2020, 92, 4647–4655.
77. Lim, H.R.; Kim, Y.S.; Kwon, S.; Mahmood, M.; Kwon, Y.T.; Lee, Y.; Lee, S.M.; Yeo, W.H. Wireless, Flexible, Ion-Selective Electrode System for Selective and Repeatable Detection of Sodium. Sensors 2020, 20, 3297.
78. Iijima, S. Helical microtubules of graphitic carbon. Nature 1991, 354, 56–58.
79. Bandodkar, A.J.; Jeerapan, I.; You, J.M.; Nuñez-Flores, R.; Wang, J. Highly Stretchable Fully-Printed CNT-Based Electrochemical Sensors and Biofuel Cells: Combining Intrinsic and Design-Induced Stretchability.

2.3. Electronic Device

Miniaturized electronic SSDs in the form of a simple and fashionable daily-worn accessory, such as a smartwatch, can be the ideal choice for a sweat monitoring platform routine. Cao et al. introduced a smartwatch integrated with a paper-based microfluidic patch for sweat monitoring, providing a digital display of real-time detection results of potassium and sodium ions in sweat [129]. However, the SSD they demonstrated was insufficient in accomplishing the specifications for a commercial product. More endeavors and clinical studies are needed to promote smartwatch intelligence, including incorporating additional sensors such as body temperature, pulse rate, and other chemical sensors. Lin et al. developed an SSD consisting of a microfluidic valve, sensors, and a wireless flexible printed circuit board to communicate with consumer electronic devices (e.g., smartwatches and smartphones through Bluetooth) [48]. Their smartwatch application includes the following three main functions that are accessible via the main selection screen, which also displays the current time: history (which stores and displays a time series bar chart that represents the most recently recorded biomarker data), scheduled (which exhibits the configured biomarker recording schedule and the sensor selection activation command, which includes glucose and lactate), and a remote-controlled view from which the sensor activation command can be transmitted on-demand by a user who selects the required sensor section) [130][131].

Electricity generation for SSDs can be developed from battery-free systems, which offers miniaturized, lightweight, and wireless electronic devices that are more versatile under daily use. Typically, this electric energy can be retrieved from sustainable, portable, and renewable resources such as sunlight [132], human motion (biomechanical) [133], and biofuel cells (BFCs) [134] to power wireless wearable electronics. However, solar cells must be integrated with the energy storage devices or rechargeable batteries such as lithium-ion batteries, zinc-carbon batteries, and supercapacitors, which contain hazardous constituent materials and require external charging or frequent power source replacement [36][135][136]. Moreover, energy storage devices and photovoltaic cells are required to address the limitations imposed by sunlight availability and serve as an efficient and long-term source of power [137]. Rechargeable batteries are also susceptible to explosion, generate huge currents, and are short-circuited when present with sweat, posing safety concerns, which may cause skin burns. Despite solar energy, human motion and BFC are viable alternatives. Both are types of on-body energy sources that are generally available and still in their infancy. Therefore, several biomechanical and biochemical system analyses are discussed in this section to provide concepts and insight for future researchers to optimize viable, ecologically friendly energy sources for future wearable electronics and support active device operation, raising intense research interest.

Energy harvesting from human motion generates electricity, which distributes the current into sensors and electronic devices through current displacement based on mechanical triggers. This is known as a nanogenerator, which is sorted into piezoelectric nanogenerators (PENG) [124][138] and triboelectric nanogenerators (TENG) [139][140]. Mechanical energy is an independent operation and is able to control the production of external power sources. The piezoelectric material adopted in PENGs is installed between the top and bottom electrodes. The electrostatic potential is generated by piezoelectric material, inducing an electric current to flow between both the electrodes when subjected to an exerted vertical strain. The electrons' backflow creates a reversed current upon release of the strain. However, TENGs give a larger current output and can involve a wider range of material selections than PENGs, making it an excellent candidate for biomechanical energy harvesting in low-frequency human motion. Moreover, TENGs are flexible and versatile in recuperating the kinetic energy from the mechanical motion of various working modes of electrodes via the coupling of inductive and triboelectric effects [141][142], generating a flow of voltage and current. Song et al. proposed a freestanding TENG (FTENG)-powered SSD that efficiently extracts power from body motion, powering multiplexed sweat biochemical sensors and wirelessly transmitting health status tracking during exercise via Bluetooth to communicate with the user [86]. In comparison to the prior efforts of TENGs that suffer from low power intensity [143][144], their fabricated FTENG exhibited great significance in terms of mechanical and electrical reliability and stability, in which an outstanding performance in terms of real-time energy usage and longevity for wearable electronics was achieved. They proposed an efficient dielectric modulation strategy to tackle this challenge by optimizing their charge trapping capacity and surface charge density. Furthermore, the storage capacitor in the FTENG releases its stored energy when fully charged, maintaining optimum power over ultra-long charging periods to perform the measurement of practicality for wearable applications [145]. Meanwhile, some novel designs to enhance the output performance of PENGs still deserve more attention.

BFCs also carry a function as a self-powered sweat detecting system. The available target biomarkers in sweat secretion serve as fuels to transform the catalytic reaction into electrical power. Glucose [134][146][147] and lactate [148][149][150] are sweat analytes that consume biomass for electricity generation, benefiting the biocatalytic redox enzyme reaction to generate protons and electrons. Then, these charges in sweat become the external loading for the connection between the anode and cathode, producing a current intensity that is proportional to the biofuels' concentration until the BFC is completely saturated. Sweat-lactate-based wearable biofuel cells are an effective candidate for addressing power concerns, owing to the fact that

Nano Lett. 2016, 16, 721–727.

80. Emaminejad, S.; Gao, W.; Wu, E.; Davies, Z.A.; Yin Yin Nyein, H.; Challa, S.; Ryan, S.P.; Fahad, H.M.; Chen, K.; Shahpar, Z.; et al. Autonomous sweat extraction and analysis applied to cystic fibrosis and glucose monitoring using a fully integrated wearable platform. Proc. Natl. Acad. Sci. USA 2017, 114, 4625–4630.

81. Liu, H.; Gu, Z.; Zhao, Q.; Li, S.; Ding, X.; Xiao, X.; Xiu, G. Printed circuit board integrated wearable ion-selective electrode with potential treatment for highly repeatable sweat monitoring. Sens. Actuators B Chem. 2022, 355, 131102.

82. Lee, H.; Song, C.; Hong, Y.S.; Kim, M.S.; Cho, H.R.; Kang, T.; Shin, K.; Choi, S.H.; Hyeon, T.; Kim, D.H. Wearable/disposable sweat-based glucose monitoring device with multistage transdermal drug delivery module. Sci. Adv. 2017, 3, e1601314.

83. Bandodkar, A.J.; Jia, W.; Yardimci, C.; Wang, X.; Ramirez, J.; Wang, J. Tattoo-based noninvasive glucose monitoring: A proof-of-concept study. Anal. Chem. 2015, 87, 394–398.

84. Ghosh, T.; Chung, H.J.; Rieger, J. All-Solid-State Sodium-Selective Electrode with a Solid Contact of Chitosan/Prussian Blue Nanocomposite. Sensors 2017, 17, 2536.

85. Zuliani, C.; Matzeu, G.; Diamond, D. A liquid-junction-free reference electrode based on a PEDOT solid-contact and ionogel capping membrane. Talanta 2014, 125, 58–64.

86. Song, Y.; Min, J.; Yu, Y.; Wang, H.; Yang, Y.; Zhang, H.; Gao, W. Wireless battery-free wearable sweat sensor powered by human motion. Sci. Adv. 2020, 6, 9842.

87. Gao, W.; Emaminejad, S.; Nyein, H.Y.Y.; Challa, S.; Chen, K.; Peck, A.; Fahad, H.M.; Ota, H.; Shiraki, H.; Kiriya, D.; et al. Fully integrated wearable sensor arrays for multiplexed in situ perspiration analysis. Nature 2016, 529, 509–514.

88. Oh, S.Y.; Hong, S.Y.; Jeong, Y.R.; Yun, J.; Park, H.; Jin, S.W.; Lee, G.; Oh, J.H.; Lee, H.; Lee, S.S.; et al. Skin-Attachable, Stretchable Electrochemical Sweat Sensor for Glucose and pH Detection. ACS Appl. Mater. Interfaces 2018, 10, 13729–13740.

89. Bariya, M.; Shahpar, Z.; Park, H.; Sun, J.; Jung, Y.; Gao, W.; Nyein, H.Y.Y.; Liaw, T.S.; Tai, L.C.; Ngo, Q.P.; et al. Roll-to-Roll Gravure Printed Electrochemical Sensors for Wearable and Medical Devices. ACS Nano 2018, 12, 6978–6987.

90. Poletti, F.; Zanfrognini, B.; Favaretto, L.; Quintano, V.; Sun, J.; Treossi, E.; Melucci, M.; Palermo, V.; Zanardi, C. Continuous capillary-flow sensing of glucose and lactate in sweat with an electrochemical sensor based on functionalized graphene oxide. Sens. Actuators B Chem. 2021, 344, 130253.

91. Salatiello, S.; Spinelli, M.; Cassiano, C.; Amoresano, A.; Marini, F.; Cinti, S. Sweat urea bioassay based on degradation of Prussian Blue as the sensing architecture. Anal. Chim. Acta 2022, 1210, 339882.

92. Payne, M.E.; Zamarayeva, A.; Pister, V.I.; Yamamoto, N.A.; Arias, A.C. Printed, Flexible Lactate Sensors: Design Considerations Before Performing On-Body Measurements. Sci. Rep. 2019, 9, 13720.

93. Yokus, M.A.; Songkakul, T.; Pozdin, V.A.; Bozkurt, A.; Daniele, M.A. Wearable multiplexed biosensor system toward continuous monitoring of metabolites. Biosens. Bioelectron. 2020, 153, 112038.

High lactate levels can be combined with low glucose levels, promising the production of a high-power density [148]. Besides glucose and lactate, sweat ethanol has also been tested as a fuel source in the creation of wearable biofuel cells [151]. A BFC based on in situ ethanol detection usually yields real-time bioelectricity generation from alcohol drinkers' perspiration. Sweat from individuals consuming lower doses had lower alcohol absorption and excretion rates [152], leading to lower bioenergy harvesting from sweat, an important guideline for controlling alcohol ingestion for heavy drinkers. Sadly, enzymatic fuel cells cannot generate electricity for an extended period of time because many oxidation–reduction enzymes degrade rapidly with low interactions, limiting their biocatalytic activity, stability, endurance, and energy capacity. Interestingly, Ryu et al. pioneered high robustness and long-lasting perspiration-based electricity production via a wearable paper-based microbial fuel cell (MFC) made by using a spore-forming skin bacterium, Bacillus Subtilis (BS) [153]. In an extreme condition that led to the limitation of sweat, the BS formed endospores. When sweat was introduced, the BS repeatedly germinated spores to prevent their denaturation or degradation. This circumstance enabled the electrogenic capability of the BS to generate a sufficiently high-power density for a small-scale battery. Moreover, sensors powered by bacteria could be used to monitor human skin health and possibly release antibiotics, making BS a more appropriate source of energy when wound-healing devices or microneedles with transdermal drug delivery systems are present.

Recent wearable electronic devices in SSDs have incorporated wireless communication and transmission data using radio-frequency power communication technologies such as wi-fi, Bluetooth, and radiofrequency identification (RFID), which expose their users to radiation risks. However, there are currently no solid data regarding the hazards of low-level radiofrequency radiation, as chronic low-intensity radiation exposure poses unknown risks because of the lack of statistically significant effects in many studies, aside from the heating effects of excessive exposure [154]. However, when operating multiple numbers of high-power wearable or portable devices at the same time, researchers should be aware of the cumulative consequences of low-intensity radiation exposure [155]. These technologies are important in enabling the Internet-of-Things (IoT) that allows innovative sweat-sensing devices and other technology to communicate with one another over the internet. Nonetheless, everything involved with internet activity has the potential to erode user personal privacy including account details, passwords, and other vague data. Thus, user privacy must be protected using encryption schemes and personal identifiers for security purposes, whilst also maintaining safety from cyber attackers, scammers, and digital stalking. Abdulla et al. presented an IoT application in a sweating finger sensor that detected the user's emotional state by utilizing a secure two-tier platform to integrate RFID and steganography to securely store collected data in a database while also increasing real-time data collection [156]. Steganography is a technique that encrypts user data to make it more secure than ever [157]. Consumers' personal health assessments were stored in a separate database that could only be accessed by doctors and their families using RFID technology. RFID technology was used to ensure that the user can access the data only after placing their card on the reader, keeping the data in the IoT and a database.

Wearable sweat-sensing electronics have recently been established with machine learning (ML) to create smart and intelligent digital networks with wide-ranging applications in fields including healthcare monitoring, disease detection, and personalized medical treatment. An ML algorithm offers advanced tools for processing and analyzing a large volume and complexity of raw data from SSDs to improve the performance and quality of their system-level operation. This can be accomplished by combining it with statistical approaches that enable a computer to learn from past experiences/historical data, followed by the implementation of training and testing. The performance of the prediction model is measured using metrics such as mean absolute error (MAE) and standard deviation (SD). Baik et al. evaluated the performance of their colorimetric sensor by applying Pearson's correlation between actual and predicted pH values [158]. The results of this analysis were $r = 0.93$; $p < 0.01$; MAE = 0.27. These data showed that their machine-learning-based pH quantification system was highly effective for accurately screening the skin's pH and diagnosing the early signs of skin problems such as acne. They used linear regression to predict pH values from RGB value conversions. When the regression trend was linearly

94. Onor, M.; Gufoni, S.; Lomonaco, T.; Ghimenti, S.; Salvo, P.; Sorrentino, F.; Bramanti, E. Potentiometric sensor for non invasive lactate determination in human sweat. Anal. Chim. Acta 2017, 989, 80–87.
95. Furlan De Oliveira, R.; Montes-García, V.; Livio, P.A.; Begoña González-García, M.; Fanjul-Bolado, P.; Casalini, S.; Samorì, P.; Furlan De Oliveira, R.; Montes-García, V.; Livio, P.A.; et al. Selective Ion Sensing in Artificial Sweat Using Low-Cost Reduced Graphene Oxide Liquid-Gated Plastic Transistors. Small 2022, 18, 2201861.
96. Zhu, Z.; Zhong, W.; Zhang, Y.; Dong, P.; Sun, S.; Zhang, Y.; Li, X. Elucidating electrochemical intercalation mechanisms of biomass-derived hard carbon in sodium-/potassium-ion batteries. Carbon Energy 2021, 3, 541–553.
97. Mahmood, A.; Li, S.; Ali, Z.; Tabassum, H.; Zhu, B.; Liang, Z.; Meng, W.; Aftab, W.; Guo, W.; Zhang, H.; et al. Ultrafast Sodium/Potassium-Ion Intercalation into Hierarchically Porous Thin Carbon Shells. Adv. Mater. 2019, 31, 1805430.
98. Alvin, S.; Cahyadi, H.S.; Hwang, J.; Chang, W.; Kwak, S.K.; Kim, J. Revealing the Intercalation Mechanisms of Lithium, Sodium, and Potassium in Hard Carbon. Adv. Energy Mater. 2020, 10, 2000283.
99. Lyu, Y.; Zhang, Y.; Xu, L.; Zhong, L.; Sun, Z.; Ma, Y.; Bao, Y.; Gan, S.; Niu, L. Solid-Contact Ion Sensing without Using an Ion-Selective Membrane through Classic Li-Ion Battery Materials. Anal. Chem. 2021, 93, 7588–7595.
100. Sekine, Y.; Kim, S.B.; Zhang, Y.; Bandodkar, A.J.; Xu, S.; Choi, J.; Irie, M.; Ray, T.R.; Kohli, P.; Kozai, N.; et al. A fluorometric skin-interfaced microfluidic device and smartphone imaging module for in situ quantitative analysis of sweat chemistry. Lab Chip 2018, 18, 2178–2186.
101. Bandodkar, A.J.; Gutruf, P.; Choi, J.; Lee, K.; Sekine, Y.; Reeder, J.T.; Jeang, W.J.; Aranyosi, A.J.; Lee, S.P.; Model, J.B.; et al. Battery-free, skin-interfaced microfluidic/electronic systems for simultaneous electrochemical, colorimetric, and volumetric analysis of sweat. Sci. Adv. 2019, 5, eaav3294.
102. Xiao, J.; Liu, Y.; Su, L.; Zhao, D.; Zhao, L.; Zhang, X. Microfluidic Chip-Based Wearable Colorimetric Sensor for Simple and Facile Detection of Sweat Glucose. Anal. Chem. 2019, 91, 14803–14807.
103. Kim, S.; Lee, B.; Reeder, J.T.; Seo, S.H.; Lee, S.U.; Hourlier-Fargette, A.; Shin, J.; Sekine, Y.; Jeong, H.; Oh, Y.S.; et al. Soft, skin-interfaced microfluidic systems with integrated immunoassays, fluorometric sensors, and impedance measurement capabilities. Proc. Natl. Acad. Sci. USA 2020, 117, 27906–27915.
104. Jiang, N.; Yetisen, A.K.; Linhart, N.; Flisikowski, K.; Dong, J.; Dong, X.; Butt, H.; Jakobi, M.; Schnieke, A.; Koch, A.W. Fluorescent dermal tattoo biosensors for electrolyte analysis. Sens. Actuators B Chem. 2020, 320, 128378.
105. Ardalan, S.; Hosseinifard, M.; Vosough, M.; Golmohammadi, H. Towards smart personalized perspiration analysis: An IoT-integrated cellulose-based microfluidic wearable patch for smartphone fluorimetric multi-sensing of sweat biomarkers. Biosens. Bioelectron. 2020, 168, 112450.
106. Chung, M.; Fortunato, G.; Radacsi, N. Wearable flexible sweat sensors for healthcare monitoring: A review. J. R. Soc. Interface 2019, 16, 20190217.
107. Califf, R.M. Biomarker definitions and their applications. Exp. Biol. Med. 2018, 243, 213.

increasing the color values were a significant indicator of pH. Then machine-learning-based software application could then automatically measure real-time pH values. In situ based on the color displayed by the colorimetric pH monitoring of sweat. Using appropriate ML algorithms, important information about various signal characteristics can be extracted from raw data and exploited to their maximum capabilities. This would increase the intelligence of these wearable devices' functionality. Lin et al. implemented a high recognition of ML on all-fiber motion sensors (AFMS) for relatively effective and precise tracking of human motion (e.g., throat) [159]. XGBoost (XGB), k-nearest neighbor (KNN), and support vector machine (SVM) are the three machine learning models that were utilized to classify the physiological data obtained from the AFMS for the purpose of detecting throat motion. XGB's classification results were good, with few outliers, a concentrated distribution, a high mean value, and a high classification speed and accuracy. Thus, it was practicable and reliable for detecting the earliest signs of viral throat diseases, monitoring their severity, and diagnosing related symptoms. Other ML techniques for the most recent SSDs with some electronic device features are outlined in **Table 3**.

Table 3. A summary of the latest SSDs' electronic device features advancements in 2022.

SSD Forms	Types of Power Source	Sensor Involved	Wireless Communication	Commercial Product	Machine Learning	Applications	References
Smartwatch	Rechargeable LiPo battery	Temperature sensor, relative humidity sensor, glucose sensor	Bluetooth	N/A	Decision tree regression algorithm	Continuous glucose monitoring	[160]
Adhesive tape	TENG	Acoustic sensors, epidermal sensor, triboelectric sensor, heart rate sensor	Internet-of-Things (IoT)	N/A	Deep learning algorithms	Human activity monitoring, cardiovascular monitoring, acoustic-biometric applications	[161]
Smart necklace	BFC	Sodium, hydrogen, potassium, glucose sensor	Vector network analyzer (VNA)	N/A	A low-pass fast Fourier transform algorithm	Detect sweat electrolytes and glucose	[162]
Hexagonal bounding shape of microfluidic patch	N/A	Colorimetric, sodium sensor, chloride sensors	Image capture from microfluidic patch sweat metrics using smartphone	N/A	Canny edge detection algorithm, image analysis algorithms, multiple regressions	Sweating rate, total sweat loss, sweat electrolyte concentration loss	[163]
A nano-porous polyamide substrate	Battery	Cytokine sensor	N/A	N/A	Supervised discriminant factor analysis	Detect of Interleukin-31 (IL-31),	[164]

108. Pławińska, Ż.; Michalska, A.; Maksymiuk, K. Optimization of capacitance of conducting polymer solid contact in ion-selective electrodes. Electrochim. Acta 2016, 187, 397–405.

109. Nicholson, R.S. Theory and Application of Cyclic Voltammetry for Measurement of Electrode Reaction Kinetics. Anal. Chem. 2002, 37, 1351–1355.

110. Lo, T.W.B.; Aldous, L.; Compton, R.G. The use of nano-carbon as an alternative to multi-walled carbon nanotubes in modified electrodes for adsorptive stripping voltammetry. Sens. Actuators B Chem. 2012, 162, 361–368.

111. Rose, D.P.; Ratterman, M.E.; Griffin, D.K.; Hou, L.; Kelley-Loughnane, N.; Naik, R.R.; Hagen, J.A.; Papautsky, I.; Heikenfeld, J.C. Adhesive RFID Sensor Patch for Monitoring of Sweat Electrolytes. IEEE Trans. Biomed. Eng. 2015, 62, 1457–1465.

112. Zhang, Y.; Guo, H.; Kim, S.B.; Wu, Y.; Ostojich, D.; Park, S.H.; Wang, X.; Weng, Z.; Li, R.; Bandodkar, A.J.; et al. Passive sweat collection and colorimetric analysis of biomarkers relevant to kidney disorders using a

113. ... ai, L.C.; Ota, H.; ... nitoring of

114. ... , J.; Jammes, Y.; ... s:Pilocarpine ... 7, 11801.

115. ... rlier-Fargette, A.; ... or accurate

116. ... arable patch for

117. ...

118. ... us response.

119. ... ; Hou, L.; et al. ... 351.

120. ... A.A.; Zhang, F.; ... namic and

121. Imani, S.; Bandodkar, A.J.; Mohan, A.M.; Kumar, R.; Yu, S.; Wang, J.; Mercier, P.P. A wearable chemical-electrophysiological hybrid biosensing system for real-time health and fitness monitoring. Nat. Commun. 2016, 7, 11650.

122. Xiao, J.; Fan, C.; Xu, T.; Su, L.; Zhang, X. An electrochemical wearable sensor for levodopa quantification in sweat based on a metal–Organic framework/graphene oxide composite with integrated enzymes. Sens. Actuators B Chem. 2022, 359, 131586.

SSD Forms	Types of Power Source	Sensor Involved	Wireless Communication	Commercial Product	Machine Learning	Applications	References
along with serpentine gold electrodes					(DFA) linear regression model of a binary classifier	chronic skin disease	
Wristband	3.7 V LiPo battery (168 h on single charge)	Interferon-inducible protein (IP-10), tumor necrosis factor-related apoptosis-inducing ligand (TRAIL), and C-reactive protein (CRP) sensors	Bluetooth (Smartphone app)	SWEATSENSER Dx-EnLiSense	N/A	Detect simultaneously and continuously specific IP-10, TRAIL, CRP	[165]
Smartwatch	110 mAh Li-ion battery	Cortisol sensor	Bluetooth	Aptamer-FET biosensing smartwatch	N/A	Track stress level	[166]
Wristband	N/A	IL-6 sensor, pH sensor	Bluetooth	WRRIST	N/A	Detect IL-6 levels (Inflammatory biomarkers)	[167]

12 ... highly accurate ... 132489.

12 ... et al. Human

12 ... arable ... Chem. 2021,

12 ... fabricated ... 022, 368,

12 ... works integrated

12 ... mechanisms of ... 10, 045003.

12 ... Paper-based

13 ... by iontophoretic delivery of the slowly-metabolized cholinergic agent carbachol. J. Dermatol. Sci. 2018, 89, 40–51.

131. Francis, J.; Stamper, I.; Heikenfeld, J.; Gomez, E.F. Digital nanoliter to milliliter flow rate sensor with in vivo demonstration for continuous sweat rate measurement. Lab Chip 2018, 19, 178–185.

132. Zhao, J.; Lin, Y.; Wu, J.; Nyein, H.Y.Y.; Bariya, M.; Tai, L.C.; Chao, M.; Ji, W.; Zhang, G.; Fan, Z.; et al. A Fully Integrated and Self-Powered Smartwatch for Continuous Sweat Glucose Monitoring. ACS Sens. 2019, 4, 1925–1933.

133. Song, Y.; Wang, H.; Cheng, X.; Li, G.; Chen, X.; Chen, H.; Miao, L.; Zhang, X.; Zhang, H. High-efficiency self-charging smart bracelet for portable electronics. Nano Energy 2019, 55, 29–36.

134. Yu, Y.; Nassar, J.; Xu, C.; Min, J.; Yang, Y.; Dai, A.; Doshi, R.; Huang, A.; Song, Y.; Gehlhar, R.; et al. Biofuel-powered soft electronic skin with multiplexed and wireless sensing for human-machine interfaces. Sci. Robot. 2020, 5, eaaz7946.

135. Tai, L.C.; Gao, W.; Chao, M.; Bariya, M.; Ngo, Q.P.; Shahpar, Z.; Nyein, H.Y.Y.; Park, H.; Sun, J.; Jung, Y.; et al. Methylxanthine Drug Monitoring with Wearable Sweat Sensors. Adv. Mater. 2018, 30, 1707442.

136. Zhao, J.; Zha, J.; Zeng, Z.; Tan, C. Recent advances in wearable self-powered energy systems based on flexible energy storage devices integrated with flexible solar cells. J. Mater. Chem. A 2021, 9, 18887–18905.

137. Dong, P.; Rodrigues, M.T.F.; Zhang, J.; Borges, R.S.; Kalaga, K.; Reddy, A.L.; Silva, G.G.; Ajayan, P.M.; Lou, J. A flexible solar cell/supercapacitor integrated energy device. Nano Energy 2017, 42, 181–186.

138. Siddiqui, S.; Lee, H.B.; Kim, D.I.; Duy, L.T.; Hanif, A.; Lee, N.E. An Omnidirectionally Stretchable Piezoelectric Nanogenerator Based on Hybrid Nanofibers and Carbon Electrodes for Multimodal Straining

and Human Kinematics Energy Harvesting. Adv. Energy Mater. 2018, 8, 1701520.

139. Zhao, T.; Fu, Y.; Sun, C.; Zhao, X.; Jiao, C.; Du, A.; Wang, Q.; Mao, Y.; Liu, B. Wearable biosensors for real-time sweat analysis and body motion capture based on stretchable fiber-based triboelectric nanogenerators. Biosens. Bioelectron. 2022, 205, 114115.
140. Zhang, Q.; Jin, T.; Cai, J.; Xu, L.; He, T.; Wang, T.; Tian, Y.; Li, L.; Peng, Y.; Lee, C. Wearable Triboelectric Sensors Enabled Gait Analysis and Waist Motion Capture for IoT-Based Smart Healthcare Applications. Adv. Sci. 2022, 9, 2103694.
141. Wang, J.; Li, S.; Yi, F.; Zi, Y.; Lin, J.; Wang, X.; Xu, Y.; Wang, Z.L. Sustainably powering wearable electronics solely by biomechanical energy. Nat. Commun. 2016, 7, 12744.
142. Liu, D.; Yin, X.; Guo, H.; Zhou, L.; Li, X.; Zhang, C.; Wang, J.; Wang, Z.L. A constant current triboelectric nanogenerator arising from electrostatic breakdown. Sci. Adv. 2019, 5, eaav6437.
143. Chen, X.; Song, Y.; Su, Z.; Chen, H.; Cheng, X.; Zhang, J.; Han, M.; Zhang, H. Flexible fiber-based hybrid nanogenerator for biomechanical energy harvesting and physiological monitoring. Nano Energy 2017, 38, 43–50.
144. Kwak, S.S.; Yoon, H.J.; Kim, S.W. Textile-Based Triboelectric Nanogenerators for Self-Powered Wearable Electronics. Adv. Funct. Mater. 2019, 29, 1804533.
145. Yi, Q.; Pei, X.; Das, P.; Qin, H.; Lee, S.W.; Esfandyarpour, R. A self-powered triboelectric MXene-based 3D-printed wearable physiological biosignal sensing system for on-demand, wireless, and real-time health monitoring. Nano Energy 2022, 101, 107511.
146. Falk, M.; Pankratov, D.; Lindh, L.; Arnebrant, T.; Shleev, S. Miniature Direct Electron Transfer Based Enzymatic Fuel Cell Operating in Human Sweat and Saliva. Fuel Cells 2014, 14, 1050–1056.
147. Wang, C.; Shim, E.; Chang, H.K.; Lee, N.; Kim, H.R.; Park, J. Sustainable and high-power wearable glucose biofuel cell using long-term and high-speed flow in sportswear fabrics. Biosens. Bioelectron. 2020, 169.
148. Jia, W.; Valdés-Ramírez, G.; Bandodkar, A.J.; Windmiller, J.R.; Wang, J. Epidermal Biofuel Cells: Energy Harvesting from Human Perspiration. Angew. Chem. Int. Ed. 2013, 52, 7233–7236.
149. Garcia, S.O.; Ulyanova, Y.V.; Figueroa-Teran, R.; Bhatt, K.H.; Singhal, S.; Atanassov, P. Wearable Sensor System Powered by a Biofuel Cell for Detection of Lactate Levels in Sweat. ECS J. Solid State Sci. Technol. 2016, 5, M3075.
150. Koushanpour, A.; Gamella, M.; Katz, E. A Biofuel Cell Based on Biocatalytic Reactions of Lactate on Both Anode and Cathode Electrodes–Extracting Electrical Power from Human Sweat. Electroanalysis 2017, 29, 1602–1611.
151. Sun, M.; Gu, Y.; Pei, X.; Wang, J.; Liu, J.; Ma, C.; Bai, J.; Zhou, M. A flexible and wearable epidermal ethanol biofuel cell for on-body and real-time bioenergy harvesting from human sweat. Nano Energy 2021, 86, 106061.
152. Cederbaum, A.I. Alcohol metabolism. Clin. Liver Dis. 2012, 16, 667–685.

153. Ryu, J.; Landers, M.; Choi, S. A sweat-activated, wearable microbial fuel cell for long-term, on-demand power generation. Biosens. Bioelectron. 2022, 205, 114128.

154. Foster, K.R. Is Wi-Fi a Health Threat in Schools? Educ. Next 2019, 19, 28–37.

155. Ulrich, C.M.; Demiris, G.; Kennedy, R.; Rothwell, E. The ethics of sensor technology use in clinical research. Nurs. Outlook 2020, 68, 720–726.

156. Abdulla, R.; Sathish Kumar Selvaperumal, A.; Bathich, A.; Ali Khan, H.; Kumar Selvaperumal, S. IoT based on secure personal healthcare using RFID technology and steganography Wireless power transfer using conical and spiral coils View project IoT based on secure personal healthcare using RFID technology and steganography. Artic. Int. J. Electr. Comput. Eng. 2021, 11, 3300–3309.

157. Hureib, E.; Gutub, A.; Bin Hureib, E.S.; Gutub, A.A. Enhancing Medical Data Security via Combining Elliptic Curve Cryptography and Image Steganography. Int. J. Comput. Sci. Netw. Secur. 2020, 20, 1–8.

158. Baik, S.; Lee, J.; Jeon, E.J.; Park, B.Y.; Kim, D.W.; Song, J.H.; Lee, H.J.; Han, S.Y.; Cho, S.W.; Pang, C. Diving beetle-like miniaturized plungers with reversible, rapid biofluid capturing for machine learning-based care of skin disease. Sci. Adv. 2021, 7, 5695–5711.

159. Lin, S.; Hu, S.; Song, W.; Gu, M.; Liu, J.; Song, J.; Liu, Z.; Li, Z.; Huang, K.; Wu, Y.; et al. An ultralight, flexible, and biocompatible all-fiber motion sensor for artificial intelligence wearable electronics. Npj Flex. Electron. 2022, 6, 27.

160. Sankhala, D.; Sardesai, A.U.; Pali, M.; Lin, K.C.; Jagannath, B.; Muthukumar, S.; Prasad, S. A machine learning-based on-demand sweat glucose reporting platform. Sci. Rep. 2022, 12, 2442.

161. Wang, H.L.; Guo, Z.H.; Pu, X.; Wang, Z.L. Ultralight Iontronic Triboelectric Mechanoreceptor with High Specific Outputs for Epidermal Electronics. Nano-Micro Lett. 2022, 14, 86.

162. Liu, T.L.; Dong, Y.; Chen, S.; Zhou, J.; Ma, Z.; Li, J. Battery-free, tuning circuit-inspired wireless sensor systems for detection of multiple biomarkers in bodily fluids. Sci. Adv. 2022, 8, 7049.

163. Baker, L.B.; Seib, M.S.; Barnes, K.A.; Brown, S.D.; King, M.A.; De Chavez, P.J.D.; Qu, S.; Archer, J.; Wolfe, A.S.; Stofan, J.R.; et al. Skin-Interfaced Microfluidic System with Machine Learning-Enabled Image Processing of Sweat Biomarkers in Remote Settings. Adv. Mater. Technol. 2022, 7, 2200249.

164. Upasham, S.; Rice, P.; Shahub, S.; Dhamu, V.N.; Prasad, S. Passive Sweat-Based Pruritic Cytokine Detection and Monitoring System. ECS Sens. Plus 2022, 1, 031602.

165. Jagannath, B.; Pali, M.; Lin, K.C.; Sankhala, D.; Naraghi, P.; Muthukumar, S.; Prasad, S. Novel Approach to Track the Lifecycle of Inflammation from Chemokine Expression to Inflammatory Proteins in Sweat Using Electrochemical Biosensor. Adv. Mater. Technol. 2022, 7, 2101356.

166. Wang, B.; Zhao, C.; Wang, Z.; Yang, K.A.; Cheng, X.; Liu, W.; Yu, W.; Lin, S.; Zhao, Y.; Cheung, K.M.; et al. Wearable aptamer-field-effect transistor sensing system for noninvasive cortisol monitoring. Sci. Adv. 2022, 8, 967.

167. Noushin, T.; Tabassum, S. WRRIST: A wearable, rapid, and real-time infection screening tool for dual-mode detection of inflammatory biomarkers in sweat. In Microfluidics, BioMEMS, and Medical Microsystems XX; SPIE: Bellingham, WA, USA, 2022; Volume 11955, p. 1195502.